

Thermodynamic parameters of $\text{HgBa}_2\text{Ca}_2\text{Cu}_3\text{O}_{8-x}$ from high-field magnetization

Mun-Seog Kim* and Myoung-Kwang Bae

Department of Physics, Pohang University of Science and Technology, P.O. Box 125, Pohang 790-784, South Korea

W. C. Lee

Department of Physics, Sook Myung Women's University, Seoul 140-742, South Korea

Sung-Ik Lee

*Department of Physics, Pohang University of Science and Technology, P.O. Box 125, Pohang 790-784, South Korea
and Physics Division, Research Institute of Industrial Science and Technology, Pohang, South Korea*

(Received 6 September 1994)

We have measured the temperature dependence of reversible magnetization of grain-aligned $\text{HgBa}_2\text{Ca}_2\text{Cu}_3\text{O}_{8-x}$ high- T_c superconductors with external magnetic field parallel to the c axis. Our data show the crossover of the magnetization below the superconducting onset temperature, which indicates a dominant vortex fluctuation. Except this vortex fluctuation region, reversible magnetization data could be described by using Hao and Clem's model. From the analysis magnetization curve based on this model, the thermodynamic critical field $H_c(T)$ and Ginzburg-Landau parameter $\kappa = 118$ were extracted. Also, we obtained the superconducting parameters; the penetration depth $\lambda_{ab}(0) = 2060 \text{ \AA}$, coherence length $\xi_{ab}(0) = 18 \text{ \AA}$, and the zero-temperature upper critical field $H_{c2}(0) = 108 \text{ T}$.

Since the discovery of high-temperature superconductors in Hg-based copper oxides,¹ various forms of mercury cuprate²⁻⁴ have been synthesized. These materials have the highest transition temperature known for layered Cu-O materials.

In our previous works,^{5,6} we synthesized the high-purity polycrystalline $\text{HgBa}_2\text{Ca}_2\text{Cu}_3\text{O}_{8-x}$ superconductor by the freeze-drying method, investigated the temperature dependence of reversible magnetization for a grain-aligned sample, and elucidated the vortex fluctuation effect.⁷ Just below T_c , vortices are thermally distorted due to the weak interlayer coupling and form two-dimensional pancake vortices.⁷ This feature is reflected by a crossover of the magnetization $M(T)$ curves at $T = 128 \pm 1 \text{ K}$. But the vortex fluctuation model is based on the London model⁸⁻¹⁰ for reversible magnetization of high- κ type-II superconductors which is valid in restricted field regions ($H_{c1} \ll H \ll H_{c2}$). In a mixed state of a superconductor, the London model, however, only accounts for the electromagnetic energy density F_{em} for the region outside the vortex core; the core energy density F_{core} due to depression of the order parameter to zero on the axes is ignored. But the contribution of F_{core} to the magnetization is significant in a high field, because the increase in magnetization is mainly associated with F_{core} .¹¹

This paper reports the experimental results on reversible magnetization outside vortex fluctuation region for a grain-aligned $\text{HgBa}_2\text{Ca}_2\text{Cu}_3\text{O}_{8-x}$ sample. We have analyzed reversible magnetization curves in the range $110 \text{ K} \leq T \leq 124 \text{ K}$ by using the model of Hao *et al.*¹² Since the model of Hao *et al.* accounts for, in addition to the electromagnetic energy terms, the core en-

ergy terms in calculating the free energy, this model offers more reasonable thermodynamic parameters for magnetization in this temperature region. From this analysis, the Ginzburg-Landau parameter κ and thermodynamic critical field $H_c(T)$, penetration depth λ_{ab} , coherence length ξ_{ab} , and upper critical field at $T = 0 \text{ K}$ were obtained.

The sample was synthesized according to the procedure given in Ref. 5. The $\text{Ba}_2\text{Ca}_2\text{Cu}_3\text{O}_x$ precursor material was mixed with HgO and pressed into a pellet. A pellet of nominal composition $\text{HgBa}_2\text{Ca}_2\text{Cu}_3\text{O}_x$ was placed inside an alumina tube and then inside a thick-walled quartz tube. The sample was heated for 5 h at 900°C and then cooled to room temperature. The oxygenation was carried out in flowing oxygen at 300°C for 20 h. To obtain a c -axis-aligned sample, the method of Farrell *et al.*¹³ was employed. The powders were aligned in epoxy with an external magnetic field of 7 T. The alignment was confirmed by an x-ray-diffraction (XRD) experiment. The full width at half maximum (FWHM) of the rocking curve was less than 1° . The temperature dependence of the magnetization was measured by using a superconducting quantum interference device (SQUID) magnetometer (MPMS, Quantum Design). We repeated the measurement in zero-field-cooled and field-cooled conditions at various magnetic fields. Weak temperature-dependent contributions originated from the epoxy and the paramagnetic impurities were subtracted from the observed values by fitting the magnetization curve at a high-temperature region ($200 \text{ K} < T < 250 \text{ K}$) by $(C/T + \chi_0)$.

The dimensionless Ginzburg-Landau free energy¹⁴ per unit volume over cross-sectional area A in a plane perpendicular to the vortices, measured relative to that of

the Meissner state, can be expressed as

$$F = \frac{1}{A} \int d^2\rho \left[\frac{1}{2}(1-f^2)^2 + \frac{1}{\kappa^2}(\nabla f)^2 + f^2 \left(a + \frac{1}{\kappa} \nabla \gamma \right)^2 + b^2 \right]. \quad (1)$$

In this integral, the first two terms represent the core energy density and the last two terms represent the electromagnetic energy density. f and γ are the normalized magnitude and phase of the order parameter

$\Psi = \Psi_0 f e^{i\gamma}$. In this dimensionless equation, length ρ , magnetic field, and free energy are normalized by penetration depth λ , $\sqrt{2}H_c$, and $H_c^2/4\pi$, respectively, where H_c is the thermodynamic critical field. Hao *et al.* assume for the order parameter a trial function¹² as follows:

$$f = \frac{\rho}{(\rho^2 + \xi_v^2)^{1/2}} f_\infty, \quad (2)$$

where ξ_v and f_∞ are variational parameters representing the effective core radius of a vortex and the depression in the order parameter due to the overlapping of vortices, respectively. The dimensionless magnetization $-4\pi M'$ is given by

$$-4\pi M' = \frac{1}{2} \frac{\partial}{\partial B} (F - B^2)_{f_\infty, \xi_v} \quad (3)$$

$$= \frac{\kappa f_\infty^2 \xi_v^2}{2} \left[\frac{1-f_\infty^2}{2} \ln \left(\frac{2}{B\kappa\xi_v^2} + 1 \right) - \frac{1-f_\infty^2}{2+B\kappa\xi_v^2} + \frac{f_\infty^2}{(2+B\kappa\xi_v^2)^2} \right] + \frac{f_\infty^2(2+3B\kappa\xi_v^2)}{2\kappa(2+B\kappa\xi_v^2)^3} + \frac{f_\infty}{2\kappa\xi_v K_1(f_\infty\xi_v)} \left[K_0[\xi_v(f_\infty^2+2B\kappa)^{1/2}] - \frac{B\kappa\xi_v K_1[\xi_v(f_\infty^2+2B\kappa)^{1/2}]}{(f_\infty^2+2B\kappa)^{1/2}} \right], \quad (4)$$

where $K_n(x)$ is a modified Bessel function of n th order. The first two terms denote the core energy contribution to magnetization. The last term denotes the contribution of the electromagnetic energy.

Two suitable variational parameters f_∞ and ξ_v to minimize the free energy for arbitrary B and κ are approximately written as

$$f_\infty^2 = 1 - \left[\frac{B}{\kappa} \right]^4, \quad (5)$$

$$\left[\frac{\xi_v}{\xi_{v0}} \right]^2 = \left[1 - 2 \left(1 - \frac{B}{\kappa} \right)^2 \frac{B}{\kappa} \right] \left[1 + \left(\frac{B}{\kappa} \right)^4 \right], \quad (6)$$

for the cases of $\kappa > 10$ with $\kappa\xi_{v0} = \sqrt{2}$. This model was further extended to include anisotropy by using an effective-mass tensor.

Figure 1 shows the temperature dependence of the reversible magnetization of $\text{HgBa}_2\text{Ca}_2\text{Cu}_3\text{O}_{8-x}$ for various external magnetic fields parallel to the c axis. The obvious feature in Fig. 1 is the crossover of magnetization curves near $T = 128$ K. As mentioned above, this originates from the vortex fluctuation effect.^{6,7} For a theoretical description of our reversible magnetization data, we choose a set of data $\{-4\pi M_i, H_i\}$ ($i = 1, 2, \dots$) at a fixed temperature in temperature range $110 \text{ K} \leq T \leq 124 \text{ K}$ as shown in the inset of Fig. 1. If the proper value of κ is chosen, then $-4\pi M(H)$ curves could be represented to a universal curve with a scaling factor $\sqrt{2}H_c(T)$, consistent with Eq. (4). Our best fit gives $\kappa = 118 \pm 8$. Figure 2 shows $-4\pi M' = -4\pi M/\sqrt{2}H_c(T)$ versus $H' = H/\sqrt{2}H_c(T)$ of the experimental data and theoretical fitting. For each temperature, all data are collapsed onto a single curve. Figure 3 shows $H_c(T)$ obtained from the above analysis versus temperature, and a fit to the BCS temperature dependence of $H_c(T)$,¹⁵

$$\frac{H_c(T)}{H_c(0)} = 1.7367 \left[1 - \frac{T}{T_c} \right] \left[1 - 0.2730 \left(1 - \frac{T}{T_c} \right) - 0.0949 \left(1 - \frac{T}{T_c} \right)^2 \right], \quad (7)$$

which yields $H_c(0) = 5.877 \times 10^3 \pm 52$ Oe with $T_c =$

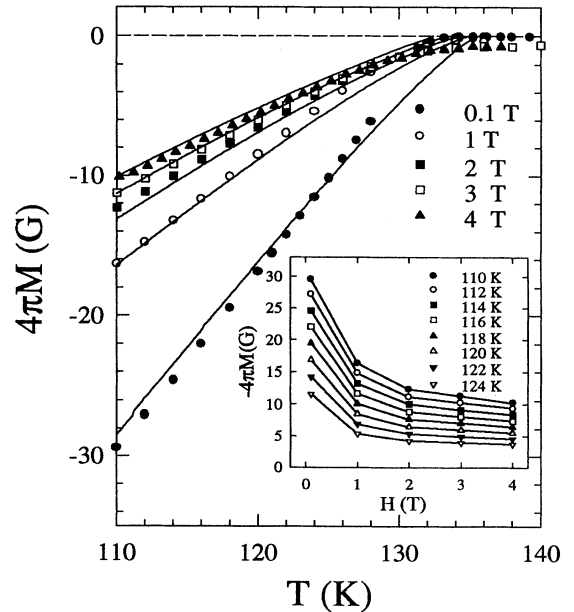


FIG. 1. Temperature dependence of reversible magnetization $4\pi M(T)$ with the theoretical curves (solid line) for $\text{HgBa}_2\text{Ca}_2\text{Cu}_3\text{O}_{8-x}$ for $H \parallel c$. Inset: magnetization versus magnetic field at various temperature.

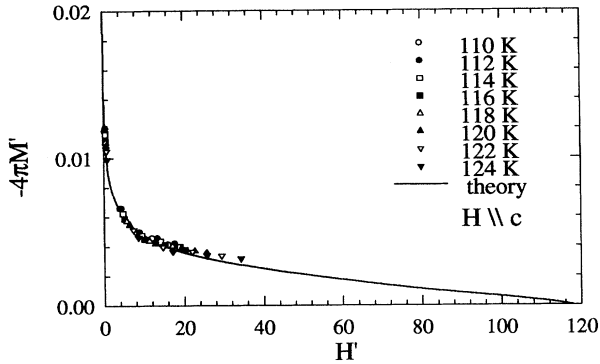


FIG. 2. The curves of $-4\pi M(H)$ scaled by $\sqrt{2}H_c(T)$. Solid line represents the universal curve by the model of Hao *et al.* with $\kappa = 118$.

135.7 ± 0.2 K. From a good fit of $H_c(T)$ by using Eq. (7), we expect that the temperature dependence of $H_c(T)$ by BCS theory is valid in our sample. And the theoretical curves of $-4\pi M(T)$ are obtained using $-4\pi M(T) = -4\pi M'(H)\sqrt{2}H_c(T)$ and Eq. (7) at constant H . The solid line of Fig. 1 shows calculated $-4\pi M(T)$. We note that the experimental data deviate from the theoretical curve for the temperature range $124 \text{ K} \leq T \leq T_c$. We conjecture that this is due to the influence of the vortex fluctuation effect, which gets more important as the temperature increases to near the T_c .⁷ In the vortex fluctuation region $124 \text{ K} \leq T \leq T_c$, the contribution of the distortion of the vortices lattice to the free energy should be considered in order to describe $-4\pi M(H, T)$ properly. However, for $110 \text{ K} \leq T \leq 124 \text{ K}$, the vortex fluctuation effect could be ignored compared with F_{em} and F_{core} .

According to the relation $H_{c2}(T) = \sqrt{2}\kappa H_c(T)$, the upper critical field slope $(\partial H_{c2}/\partial T)_{T_c} = -1.15 \pm 0.02$ T/K is estimated. The slope can be used to estimate the upper critical field at $T = 0$ by using the formula¹⁶

$$H_{c2}(0) = 0.5758 \left[\frac{\kappa_1(0)}{\kappa} \right] T_c \left| \frac{\partial H_{c2}}{\partial T} \right|_{T_c}. \quad (8)$$

In the dirty limit $\kappa_1(0)/\kappa = 1.20$,¹⁷ while in the clean limit¹⁸ $\kappa_1(0)/\kappa = 1.26$. From this formula, $H_{c2}^c(0)$ is estimated 108.1 ± 1.6 T assuming the dirty limit and 113.5 ± 1.7 T assuming the clean limit. And the upper critical field is related to the coherence length by $H_{c2}^c(0) = \phi_0/2\pi\xi_{ab}^2(0)$. The calculated $\xi_{ab}(0)$ is 17.5 ± 0.14 Å in the dirty limit. And $\lambda_{ab}(0) = 2059 \pm 15$ Å is extracted from $\kappa = \lambda/\xi$.

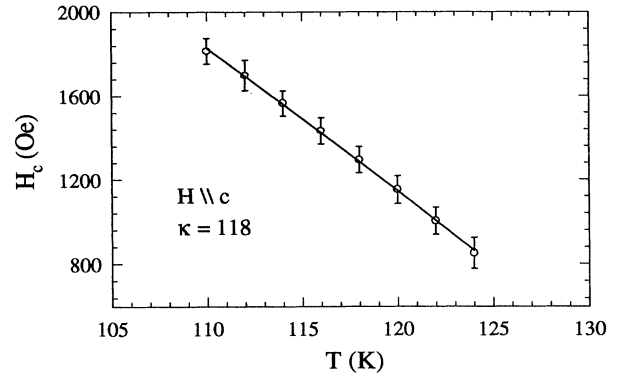


FIG. 3. Temperature dependence of thermodynamic critical field $H_c(T)$ obtained from the theoretical fitting. Solid line represents the BCS temperature dependence of $H_c(T)$.

In the model of Hao *et al.*, only high-magnetic-field magnetization is used for the analysis for the temperature range $110 \text{ K} \leq T \leq 124 \text{ K}$, where the vortex fluctuation effect can be ignored. Comparing our values with those from the vortex fluctuation analysis,⁶ our $\kappa = 118$ and $H_{c2}(0) = 108$ T are, somewhat, larger than those of the latter analysis. That inconsistency might result from the uncertainty in subtracting the magnetic impurity background. However, recalling that the model of Hao *et al.* is based on high-magnetic-field magnetization and all carriers are confined at the lowest Landau orbit in a high magnetic field,¹⁹ our values are consistent with high-magnetic-field scaling results.²⁰

Our derived $\kappa = 118$ for $\text{HgBa}_2\text{Ca}_2\text{Cu}_3\text{O}_{8-x}$ is much larger than Y-123.¹² But it is known that κ is proportional to λ/ξ in the clean limit and λ/l in the dirty limit.⁹ As Eilenberger¹⁸ pointed out previously, κ might depend not only on λ/ξ , but also on the degree of anisotropy in the impurity scattering. In another sense, κ reflects the different degree of sensitivity of the various magnetic properties of a superconductor to the degree of nonlocality. Therefore, more detailed theories and experiments are needed to clarify the difference between the two systems.

In summary, we measured the high-magnetic-field magnetization for grain-aligned $\text{HgBa}_2\text{Ca}_2\text{Cu}_3\text{O}_{8-x}$ with the magnetic field parallel to the c axis. Using the model of Hao *et al.*, we obtained the Ginzburg-Landau parameter $\kappa = 118$ and upper critical field slope $(\partial H_{c2}/\partial T)_{T_c} = -1.15$ T/K, which show that $\lambda_{ab}(0) = 2060$ Å and $\xi_{ab}(0) = 18$ Å. Our derived values are consistent with those from high-magnetic-field scaling results.

*Also Department of Physics, Chungbuk National University, Cheongju 360-763, South Korea.

¹S. N. Putilin, E. V. Antipov, O. Chmaissem, and M. Marezio, *Nature* **362**, 226 (1993).

²A. Schilling, M. Cantoni, J. D. Guo, and H. R. Ott, *Nature* **363**, 56 (1993).

³L. Gao, J. Z. Huang, R. L. Meng, G. Lin, F. Chen, L. Beauvais, Y. Y. Sun, Y. Y. Xue, and C. W. Chu, *Physica C* **213**, 261 (1993).

⁴C. W. Chu, L. Gao, F. Chen, J. Z. Huang, R. L. Meng, and Y. Y. Xue, *Nature* **365**, 323 (1993).

⁵Sergey Lee, Mi-Ock Mun, Myoung-Kwang Bae, and Sung-Ik Lee, *J. Mater. Chem.* **4**, 991 (1994).

⁶Myoung-Kwang Bae, M. S. Choi, Mi-Ock Mun, Sergey Lee, Sung-Ik Lee, and W. C. Lee, *Physica C* **228**, 195 (1994).

⁷L. N. Bulaevskii, M. Ledvij, and V. G. Kogan, *Phys. Rev. Lett.* **68**, 3773 (1992).

⁸A. A. Abirikoosov, *Zh. Eksp. Teor. Fiz.* **32**, 1442 (1957) [Sov.

- Phys. JETP **5**, 1174 (1957)].
- ⁹M. Tinkham, *Introduction to Superconductivity* (McGraw-Hill, New York, 1980).
- ¹⁰P. G. de Gennes, *Superconductivity of Metals and Alloys* (Benjamin, New York, 1966).
- ¹¹Zhidong Hao and John R. Clem, Phys. Rev. Lett. **67**, 2371 (1991).
- ¹²Zhidong Hao, John R. Clem, M. W. McElfresh, L. Civale, A. P. Malozemoff, and F. Holtzberg, Phys. Rev. B. **43**, 2844 (1991).
- ¹³D. E. Farrell, B. S. Chandrasekhar, M. M. Fang, V. G. Kogan, J. R. Clem, and D. K. Finnemore, Phys. Rev. B **36**, 4025 (1987).
- ¹⁴A. L. Fetter and P. C. Hohenberg, in *Superconductivity*, edited by R. D. Parks (Marcel Dekker, New York, 1969), p. 817.
- ¹⁵J. R. Clem, Ann. Phys (N.Y.) **40**, 286 (1966).
- ¹⁶B. Mühschlegel, Z. Phys. **155**, 584 (1967).
- ¹⁷N. R. Werthamer, E. Helfand, and P. C. Hohenberg, Phys. Rev. **147**, 295 (1966).
- ¹⁸G. Eilenberger, Phys. Rev. **153**, 584 (1967).
- ¹⁹S. Ullah and A. T. Dorsey, Phys. Rev. B **44**, 262 (1991).
- ²⁰Myoung-Kwang Bae, M. S. Choi, Sergey Lee, Sung-Ik Lee, and W. C. Lee, Physica C **231**, 249 (1994).